The Utilization of High Fidelity Simulation in the Support of High Angle of Attack Flight Testing

John Ralston

Jacob Kay

Bihrle Applied Research
18 Research Drive
Hampton, VA 23666 USA

Summary

The utilization of simulation to assist in the progress of a vehicle's flight envelope expansion during flight test has been reasonably successful, as long as the flight regime examined has been below stall. In the normal flight regime, advances in the ability of the wind tunnel and predictive theory to approximate the airplane's behavior has led to the gradual reliance on simulation in uses ranging from the development of the flight control system to assisting in the test program evolution. One area that the use of simulation remains problematic, however, is its use in the stall/post stall flight regime. Recent work in the analysis of database requirements for proper characterization of post stall motions has led to the development of new dynamic testing techniques as well as new methods of implementation of these data. This paper reviews the application of these methods to the development of a high fidelity simulation database and its varied applications in the support of a high angle of attack flight test program. The success of the flight test program was ultimately reliant on the interactive use of this simulation.

Nomenclature

The units for physical quantities used herein are presented in U.S. Customary Units, unless otherwise noted.

b	Wing span, ft.
C_l	Rolling-moment coeff., Rolling moment/qsb
C_{lp}	Rolling moment coeff. due to roll rate
C_{lr}	Rolling moment coeff. due to yaw rate
C_n	Yawing-moment coeff., Yawing moment/qsb
C_{np}	Yawing-moment coeff. due to roll rate
C_{nr}	Yawing-moment coeff. due to yaw rate
q	Free-stream dynamic pressure, lb/ft^2
p	Roll rate
r	Yaw rate
V	Free-stream velocity, ft/sec
V_T	Velocity vector
α	Angle of attack, deg
β	Angle of sideslip, deg
Ω	Rotation vector
$\Omega b/2V$	Spin coeff., positive for clockwise spin
ω	Angular velocity about wind axis, deg/sec

Subscripts:

Basic	Coeff. effects obtained from basic airframe
Dyn	Dynamic damping increment
Mod	Oscillatory residual (applied to the forced oscillation term) from the Kalviste technique
Tot	Total coefficient

Introduction

The use of airplane simulation has an extensive history in the training community, which has used simulator databases that have traditionally evolved well after the subject airplane has flown. The math models used to describe these configurations were generally very simple, derivative based, and usually hand adjusted by engineers, guided by pilots' subjective inputs and flight test results. As the expense of flight test has increased proportionally with the cost of military fighters, and with the introduction of automatic flight controls, the need and importance of developing high fidelity simulations prior to flight has also increased. Successful utilization of simulation in the high angle of attack region, typified by non-linear and non-symmetric aerodynamic characteristics, would significantly enhance the safety of the flight test program as well as permit the timely optimization of flight control systems attempting to maneuver post stall. Even though improvements in computational power have permitted increased model complexity over earlier rudimentary data, in virtually all recent applications, the simulation's confidence level drops dramatically as the vehicle enters the stall condition and

beyond. Training simulations, with the benefit of flight test data and pilot comments, have also rarely provided anything more than limited representation of stall/post-stall behavior. In many cases, the use of non-representative aerodynamic data sets have required the engineer to artificially manipulate the data in an attempt to provide an appropriate response for a given departure. Traditional linear parameter extraction techniques, frequently used at low angles of attack to refine or improve simulation response, do not cope well with the highly non-linear aerodynamic characteristics that occur in stall and beyond. As a result, the use of simulation to provide the maneuver checkout, pilot familiarization and other safety related support tasks, as well as supporting post stall flight control system development, has been limited and problematic.

There have been many recent attempts to improve the modeling of the airplane's behavior in the stall/post-stall region[1,2,3,4] and ultimately improve the simulation's predictive capabilities for flight control development, flight test, and training. Most of these attempts have focused on the development and evolution of large non-linear databases. Further, there has been increased attention on the dynamic characterization of the airplane, as well as the appropriate mechanization of these terms in the simulation. As a result of these efforts, several simulation databases have shown significant improvement in the ability to predict and model complex aircraft motions ranging from departure, post-stall motions, spins as well as other large angle excursions. While some of these simulations are currently being used to support flight test, none have been successfully used in interactive, a priori flight test support of high angle of attack flight testing.

The jet trainer configuration examined in the present study (figure 1) was an evolution of an earlier ducted fan configuration and was developed to compete in the Joint Primary Aircraft Training System (JPATS) competition. The configuration was the subject of considerable static and dynamic testing during its evolution, and these data were used as the basis for the formulation of a large angle of attack simulation dataset. The simulation itself was developed in a very compressed schedule (figure 2) in order to permit validation and re-hosting on the flight test site's simulation facility. The following discussion reviews the development, deployment and interactive use of this large angle, non-linear simulation in a high angle of attack flight test program.

Discussion

Development of Test Techniques, Implementation

As discussed above, the evolution of the simulation and its usefulness in high angle of attack simulation has evolved from earlier attempts to use flight extracted increments overlaid on a simple linear model, to the incorporation of more complex non-linear data sets. The recent successful application of these data sets shared the general approach to the database development, and these were used in the a priori application discussed herein: the key points are summarized below:

1) The most important requirement to improve the fidelity of the simulator is the correct representation of the static data. This rather intuitive statement implies the modeling of all static dependencies for both the basic airframe, as well as control effects. Past simulation models have relied on minimal definition of the basic airplane characteristics, i.e., linearized stability derivatives derived from small sideslip data. A more appropriate model incorporates a fully non-linear database with sideslip effects modeled through a sideslip range appropriate for modeling departure and post stall motions, typically out to 30° β or more (see figure 3 illustrating a sideslip effect at 0° angle of attack taken from wind tunnel data[4]). Control surface effects have also been highly simplified, but non-linear variation with deflection, sideslip, and the effect of other controls must be identified and incorporated in the database (figure 4 illustrates how the effect of sideslip and symmetric tail deflection can change the effect of differential tail in yaw from proverse to adverse in the stall region[5]). The identification of all of the basic airplane and control functionalities requires a comprehensive wind tunnel test program, and the data manipulation tools to compile this data into simulation data tables.

2) The wind tunnel acquisition of the required dynamic data (frequently omitted and the source of considerable post flight "adjustments") is also a significant requirement for the modeling of post stall motions. Analysis of the database requirements based on flight test motions[4] have shown that as the airplane departs from coordinated to uncoordinated flight, into spins and through recovery, the vehicle transitions through a range of wind axis and body axis centered rate excursions. Further, representation of the rate damping required is not adequately described by relying solely on small perturbation body axis rate derivatives. These motions require the use of wind axis damping (rotary balance test data) as well as body axis damping data collected at test conditions representative of the flight motions and expressed as a function of all

appropriate dependencies (i.e. rate, sideslip, controls, etc.)

3) The use of both body axis and wind axis damping data requires an appropriate method of mechanizing these two sets of dynamic data. Traditional mechanization has used the body axis rate derivatives multiplied by the total body rate and the incremental moment is summed as shown in the example below:

$$\Delta Cl_{dyn} = C_{lr} * rb/2V + C_{lP} * pb/2V$$

However, the assumption of linearity for the small perturbation data does not apply in the stall region. Moreover, independently tested body axis rate terms cannot be summed to represent a motion that excites both rates simultaneously anywhere other than at low angle of attack. A more appropriate mechanization scheme, as proposed by Kalviste[6], distributes the aerodynamic damping effects based on the relation of the airplane motion to the actual wind-tunnel test motions used to derive the various damping terms. This is determined by examining the relative position of the velocity vector (V_T) and the rotation vector (Ω). In the simplest terms, when the two vectors are aligned, i.e., in a coordinated rolling maneuver, the damping terms utilized would come from the rotary balance test data since the test motion is a velocity vector roll. When the rotation vector lies on either the x or z body-axes, the dynamic damping would be derived from either the body axis roll or yaw rate damping data respectively, again, because these motions are replicated by the test technique. For conditions where the rotation vector lies between these axes and the velocity vector, the dynamic damping is allocated by resolving the rotation vector (Ω) between the velocity vector (V_T) and the adjacent body axis, as shown in Figure 5. This mechanization has been successfully used in a number of high angle of attack simulation models to date[5,7], and was recommended for this particular application.

Application of Methods to Trainer Configuration

The utilization of this approach for this configuration centered around the acquisition of the needed aerodynamic test data. The wind tunnel test programs developed specifically addressed the effects of the basic configuration, effects of controls, Mach effects, and dynamic characteristics through test entries as shown in Table 1. Testing in the Rockwell Trisonic facility identified the basic low angle of attack stability levels and control effects, and was the primary source of any Mach effects that influenced these characteristics. More extensive entries in the Convair 7x10 low speed tunnel resulted in an expanded angle of attack and sideslip envelope with a greater emphasis on control power evaluations as well. A later entry was also used to assess the effects of several configuration modifications proposed later in the flight test program.

Several low speed test entries were undertaken at the Bihrle Applied Research Large Amplitude Multi-Purpose (LAMP) test facility. The flexibility of this facility permitted the acquisition of a substantial range of low speed test data ranging from basic static configuration characteristics at high angles of attack and sideslip through the collecting of both body axis and wind axis damping terms. The static and dynamic data collected in these tests also examined numerous control dependencies and interactions as well. The wind axis damping data (rotary balance data) was collected for a range of non dimensional rates ($\Omega b/2V$) from 0 to ±0.3, angles of attack from -30° to +90°, and sideslip angles through ± 30°. Control effects in the dynamic conditions were also examined. Body axis damping data were collected for the basic configuration at a number of oscillation frequencies and amplitudes. The tested non-dimensional rates (e.g., pb/2V values of 0.02, 0.04) and amplitudes (±10° and higher) were chosen to better represent the uncoordinated motion conditions typical of departure than those used in most previous test matrices (e.g. pb/2V < 0.01, amplitude of ±5 or less).

A later test entry was made to collect the necessary description of several configuration modifications. The testing conducted on these modifications ranged from static to both wind axis and body axis damping dynamic conditions.

The complexity of compiling this extensive wind tunnel database into a structure suitable for a simulation has traditionally been one of the factors driving engineers to simplify the simulation aerodynamic model. In order to take advantage of this more comprehensive database, the development of data plotting, analysis, and manipulation tools were required in order to ensure all functionalities are properly modeled and included. To support model development of this type, an extensive data manipulation tool set has been developed to permit the rapid maneuvering of test data into data structures appropriate for simulation modeling. These tools allow the transformation of multiple coefficient wind tunnel data formats into a formal single coefficient simulation data table and subsequently, any matrix operation required on this table, including graphical database editing, is permissible. Using these tools, the simulation aerodynamic database was developed, validated, and transferred to the flight test facility within two months following the end of the last tunnel entry.

An example of the subsequent aerodynamic database structure is shown in the equation below portraying the yawing moment buildup:

$$C_{n\,TOT} = C_{n\,BASIC}(\alpha, \beta, M) + DC_{n\,\delta a}(\alpha, \beta, \delta a, M) + DC_{n\,\delta r}(\alpha, \beta, \delta r, M) + DC_{np}(\alpha, Pb/2v) \times P_{MOD} b/2v + DC_{nr}(\alpha, Rb/2v) \times R_{MOD} b/2v + DC_{n\,ROTATION}(\alpha, \Omega b/2V * SGN(\beta), |\beta|) \times SGN(\beta)$$

The coefficient is the sum of the basic airplane stability with effects of aileron, rudder, body axis and wind axis damping. The non-linear sideslip effects are extended through 30° of sideslip for all components and are non-symmetrically modeled for both the basic airplane and the lateral directional controls. The wind axis damping data is expressed as a non-linear function of angle of attack, rotation rate, and sideslip. The body axis damping terms are expressed as a function of angle of attack and the non-dimensional rates. While the coefficient buildup is straight forward for this relatively simple geometry, considerable complexity and database range are incorporated in the coefficient components and their breakpoints. This is the simulation structure that was sent to the flight test center at the outset of the high angle of attack flight test program.

Use of Simulation in Support of High Angle of Attack Flight Test

Initial evaluations of the simulation spin entry, developed spin, and recoveries revealed several key characteristics. Spin entries were best accomplished using elevator and rudder alone. Aileron inputs during the departure, either in the direction of the spin or against, adversely effected the departure and transition into a developed spin, primarily because of aileron roll control power that persists through the stall. Spin entry was thus most effectively accomplished with aft stick and pro-spin rudder. These conclusions were corroborated with flight test experience. Figure 6 exhibits a typical aft stick and rudder entry with the subsequent departure motions followed by transition to a developed spin as predicted by the original simulation.

The original developed spin, as shown in figure 6, is characterized by considerable roll oscillations superimposed on the spinning motion, resulting in significant angle of attack and sideslip excursions. A flight test spin for the same loading and similar entry condition is shown in figure 7. As seen in this figure, the entry and developed spin exhibit very similar characteristics with the phase and amplitude of the oscillations exhibited during the spin matching very closely to those observed in the spin simulation. The spin turn rates and the body axis rate excursions also match very closely. Following neutralization of controls, recovery is immediate because of the high level of yaw damping afforded by the T-tail configuration.

The confidence provided by the immediate correlation of the flight and simulation results permitted a number of configurational effects to be examined and reviewed concurrent with the flight test program. These ranged from the effects of c.g., to the evaluation of inertial uncertainties and their effect on the spin characteristics, to an evaluation of engine gyroscopic effects on the spin simulation. This last evaluation arose because of observed differences between the left and right spin behavior during flight test on the original configuration. Further evaluation of the flight and wind tunnel data revealed that the post stall asymmetric aerodynamic characteristics rather than engine gyroscopic effects were primarily responsible for this asymmetric behavior.

A simulation environment that utilizes the database manipulation tools in conjunction with integrated flight test validation capabilities was used to perform engineering analysis concurrent with the flight program. A flight validation tool used heavily during the flight program was an integrated analog matching capability, referred to as “Overdrive” in the following discussion. The diagram in figure 8 details the general operation. Following importation of the flight test file into the simulation, two operations were performed. The flight test angular rates were differentiated to obtain the angular accelerations. The angular accelerations and the linear accelerations could be resolved into their aerodynamic components following removal of the inertial effects, resulting in an aerodynamic coefficient time history extracted from flight. At the same time, the simulation data set was exercised using all the state variables taken from flight test to provide the dependent variables used in the data table look-ups. The resulting file contains all the incremental values that the simulation would predict for a given coefficient, saved as a function of time. This operation, driven solely by the flight test states, eliminates the propagation of errors since no integration is taking place. The simulation predicted coefficient time history (along with time histories of all the coefficient components) can be compared with the flight extracted coefficient time histories. This method permits rapid identification of mismatches between flight test and simulation. By correlating the region of mismatch with the state variable excitation and the simulation coefficient components, identification of the potential source of error is possible. Again, because of

the lack of integration, this tool can rapidly assess large quantities of flight test data to identify areas of the model that need further refinement, and is less sensitive to flight test data quality than more traditional parameter extraction techniques. Initial evaluation of the flight test data with the simulation revealed generally good correlation between the simulation and flight data, as would be expected based on the initial correlation noted earlier.

Evaluation of the flight test data revealed that as angle of attack excursions exceeded 30° angle of attack, a repeatable discrepancy between the flight test and simulation predicted pitching moment coefficient occurred (figure 9). Examination of the pitching moment components showed that the basic airframe pitching moment was responsible for the majority of the simulation pitching moment. The only other component of consequence, $DCm_{\delta e}$, was much smaller in comparison. Further, the increase in nose down moment consistent with the mismatch was concurrent with the variations in the basic pitching moment data. Evaluation of the test data used in the basic airplane pitch buildup, from Convair tests, show a sharp nosedown break above 30° angle of attack (figure 10). Comparison with equivalent pitch data taken from the LAMP tests do not exhibit as sharp a break. The original model used the Convair data because of the higher Reynolds number test conditions, but additional influences, potentially blockage or proximity to a tunnel surface apparently adversely effected the higher angle of attack data. When the configuration pitch characteristics seen in the LAMP test data were substituted in the simulation, the pitch matches were greatly improved above 30° angle of attack, as shown in the modified Cm plot in figure 9. This modification, along with other smaller adjustments were made very early in the flight test program, resulting in the typical Overdrive moment correlation as shown in figure 11.

Early in the flight test program, spin recoveries were seen to periodically exhibit what was referred to as a "Flick-Roll". This recovery motion, as shown in figure 12, resulted when following release of controls the airplane pitched down rapidly during a large oscillation cycle. Typically the airplane would experience a large sideslip excursion at an angle of attack where the lateral stability of the airplane would impose a very large rolling moment. Subsequent roll rates exceeded 250°/sec., as shown in figure 12. The repeated experience of these rates caused concern during the flight test program, since the effect of the high roll acceleration on the wing fuel cells was not known. Following a repetitive occurrence of this maneuver, there was discussion of stopping the test program because of safety issues. Concurrent with this experience, spin recovery procedures were being evaluated with the simulation and for the current recovery procedure, all controls released simultaneously, identical roll rate behavior was observed. Further work with the simulation revealed that maintaining aft stick following the release of the pro-spin rudder reduced the roll oscillations. After the yaw rate subsided, aft stick could be released to bring angle of attack to the normal flight regime. This recovery technique was used in the simulation and flight test time histories shown earlier in figures 5 and 6, where little roll rate buildup is experienced. Although this recovery technique required a minimal increase in time to recovery, the reduction in roll rate was judged a significant improvement, and this recovery sequence became the recommended recovery technique. Following acceptance of this control input sequence, the flight test program was permitted to proceed.

As the test program continued, the magnitude of the spin oscillations were judged to be unacceptable for a training environment. The motion of the spin was quite uncomfortable with high roll accelerations and pitch angles that oscillated from nose up to pointing straight down. A few months into the test, it was decided that an attempt to reduce the oscillations through a possible external modification would be undertaken. Parametric evaluations using the simulation had shown that the roll due to yaw rate term, C_{lr}, was a key damping characteristic influencing the spin oscillation. The value of this term, as obtained from LAMP tests (figure 13) went unstable in the post-stall region and it was this characteristic that produced the spin oscillations. When the term was modified to remain positive, a much smoother spin resulted (as shown in figure 14, in comparison to figure 7). Subscale free spin testing conducted at NASA Langley revealed that the addition of forebody strakes had the effect of reducing the spin oscillations. As a consequence of these results, additional tests on these and other modifications were conducted at Convair and LAMP to acquire the required simulation database. LAMP dynamic tests showed the sensitivity to strake position and length on their ability to influence C_{lr}, as shown in the plot of figure 13. Limited visualization and component testing suggested that the vorticity shed from the strakes influenced the wing's contribution to this damping term. Spin simulation using the static and dynamic test data indicated that longer strake length would be required in order to minimize the spin oscillations, rather than the shorter length originally selected. These results were verified in flight, where smooth spins required the longer strake. A typical spin obtained with this configuration is shown in the flight test data of figure 15. This behavior was judged to be a

very satisfactory for training with good entry, spin and recovery characteristics and became the designated baseline.

Conclusions

The application of comprehensive static and dynamic test data with innovations in the method of mechanizing the data has permitted the extensive simulation support of a high angle of attack flight test program. The support function, using a flexible simulation environment to rapidly enhance simulation fidelity, permitted the real time analysis of loading, entry conditions, and recovery techniques. The use of the simulation ultimately had a significant impact on the safety and the cost effectiveness of exploring this high risk portion of the flight test program. Simulation analysis also proved valuable in developing and assessing the successful modification applied to reduce the spin oscillations. All of this was conducted in a very compressed timeline, but the successful integration of wind tunnel testing, simulation, and flight test, permitted a high level of productivity when dealing with complex flight test issues.

References

1. Fitzgerald, T., Ralston, J. and Hildreth, B.: Improvements to the Naval Air Warfare Center Aircraft Division's F/A-18 Subsonic Aerodynamic Model, AIAA94-3400, August 1994.

2. Jaramillo, P.,Ralston, J.: Flight Test Analysis and Simulation of the F-18D Falling Leaf Motion, AIAA96-3371.

3. Ralston, J., Dickes, E.: Application of Dynamic Data in Aircraft Simulation, BAR 95-1, Jan. 1995.

4. O'Connor, C., and Ralston, J.: Evaluation Of The NAWC/AD F/A-18 C/D Simulation Including Database Coverage and Dynamic Data Implementation Techniques, AIAA96-3365.

5. Ralston, John: F-16 NSI Inlet Configuration Study, Including Data, Analysis, Aerodynamic Math Modeling and Simulation, BAR 89-1, November 1989.

6. Kalviste, Juri: Use of Rotary Balance and Forced Oscillation Test Data in a Six Degrees of Freedom Simulation, AIAA Paper 82-1364, August 1982.

7. Kay, Jacob, and Ralston, John: F-15E High Angle of Attack Study, Including Data, Analysis, Aerodynamic Math Modeling, and Simulation, BAR 95-2, March 1995.

Table I. - Summary of Wind Tunnel Test Programs

Wind Tunnel	Data Range	Application in Aerodynamic Model
CONVAIR 7 X 10	-10 to 60°α, ±30°β	Static stability of baseline Control effectiveness Config. modification
Rockwell Trisonic	0 to 15°α	Static stability of baseline Mach effects
Bihrle Applied Research LAMP	Static & Rotary: -30 to 90°α, ±30°β	Static stability of baseline Control effectiveness Rotary (wind axis damping) effects Config. Modification
	Forced Oscillation: 0 to 90°α, 0°β	Body-axis roll & yaw damping Config. modification (ventral fins, strakes, etc.)

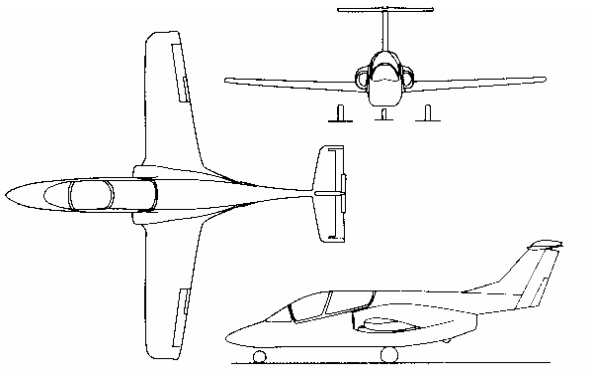

Figure 1. Three view of trainer configuration.

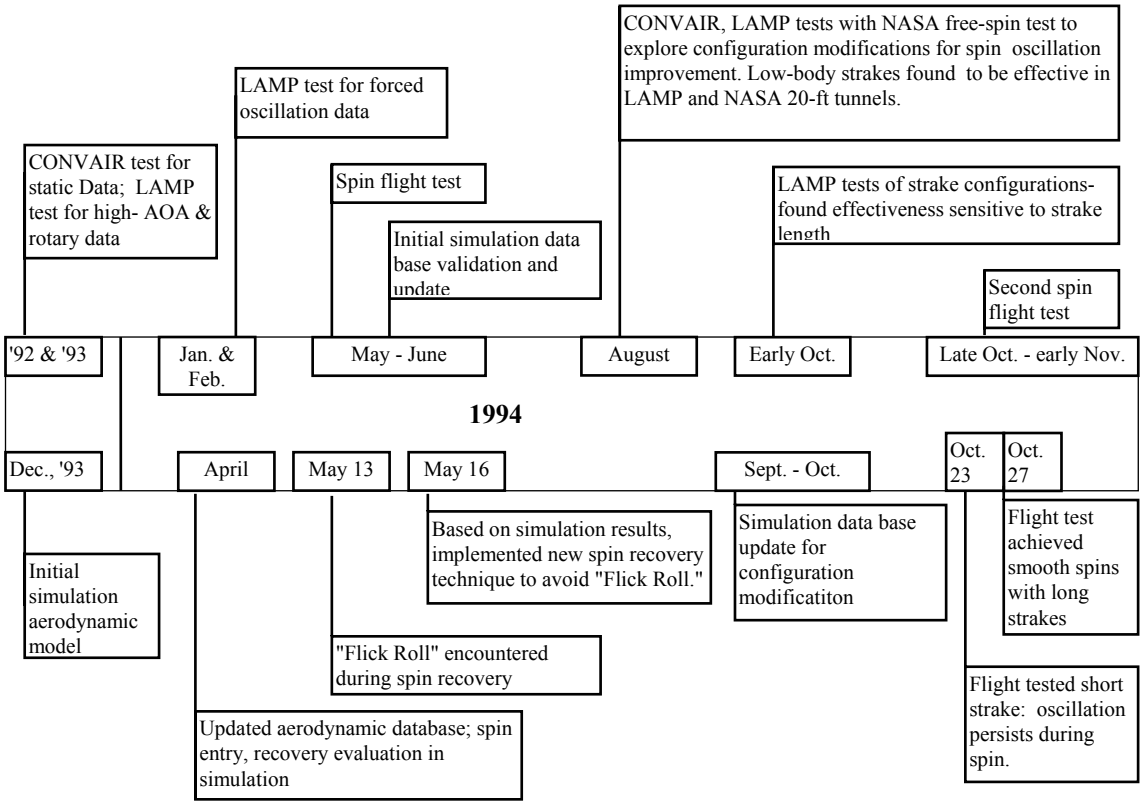

Figure 2.- Timeline of windtunnel testing, simulation and flight testing conducted on the trainer configuration

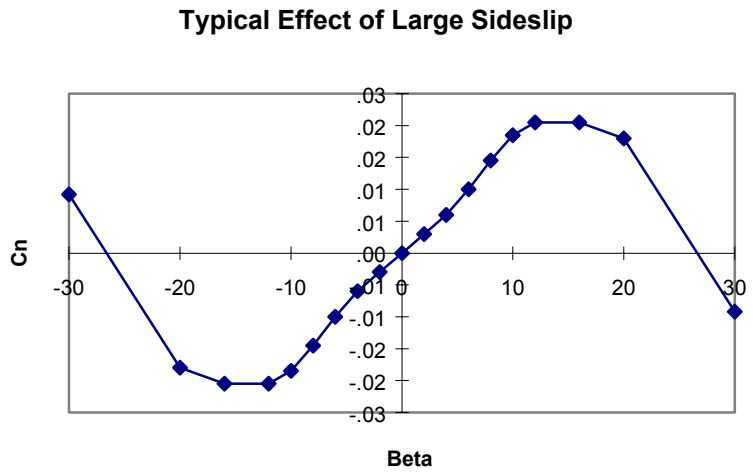

Figure 3. Effect of sideslip on yawing moment at 0° angle of attack

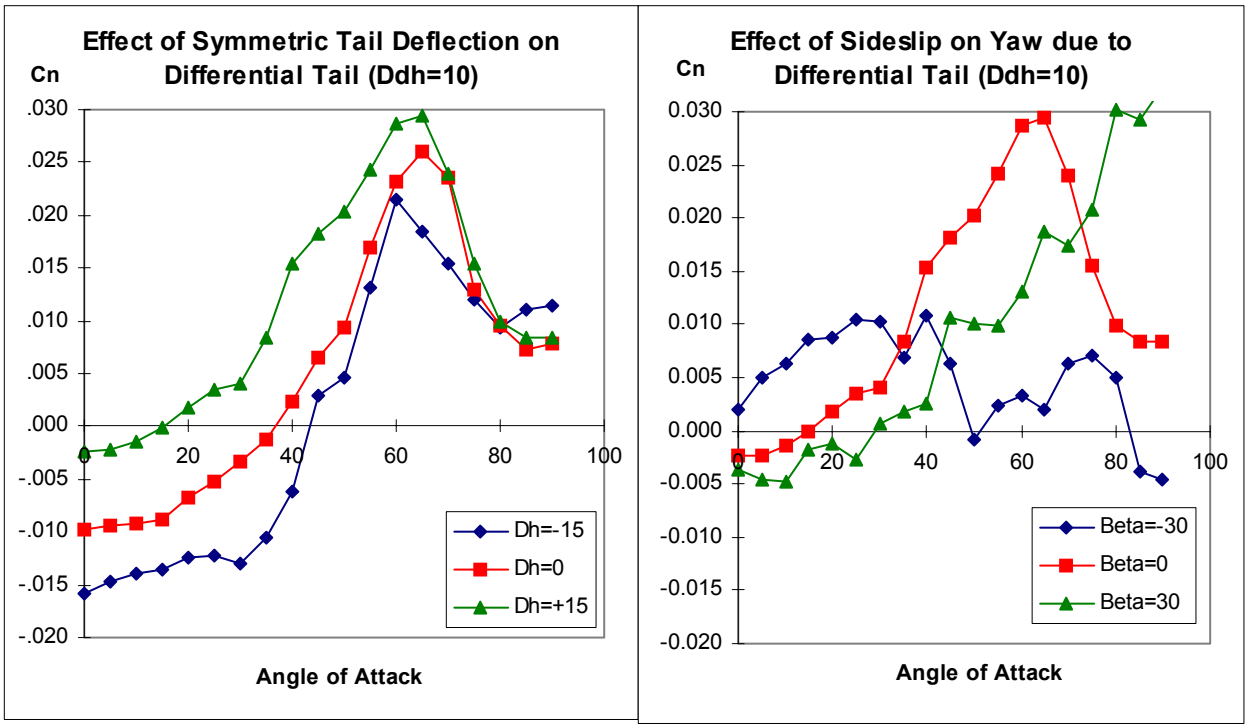

Figure 4. Effect of horizontal tail deflection and sideslip on differential tail effectiveness

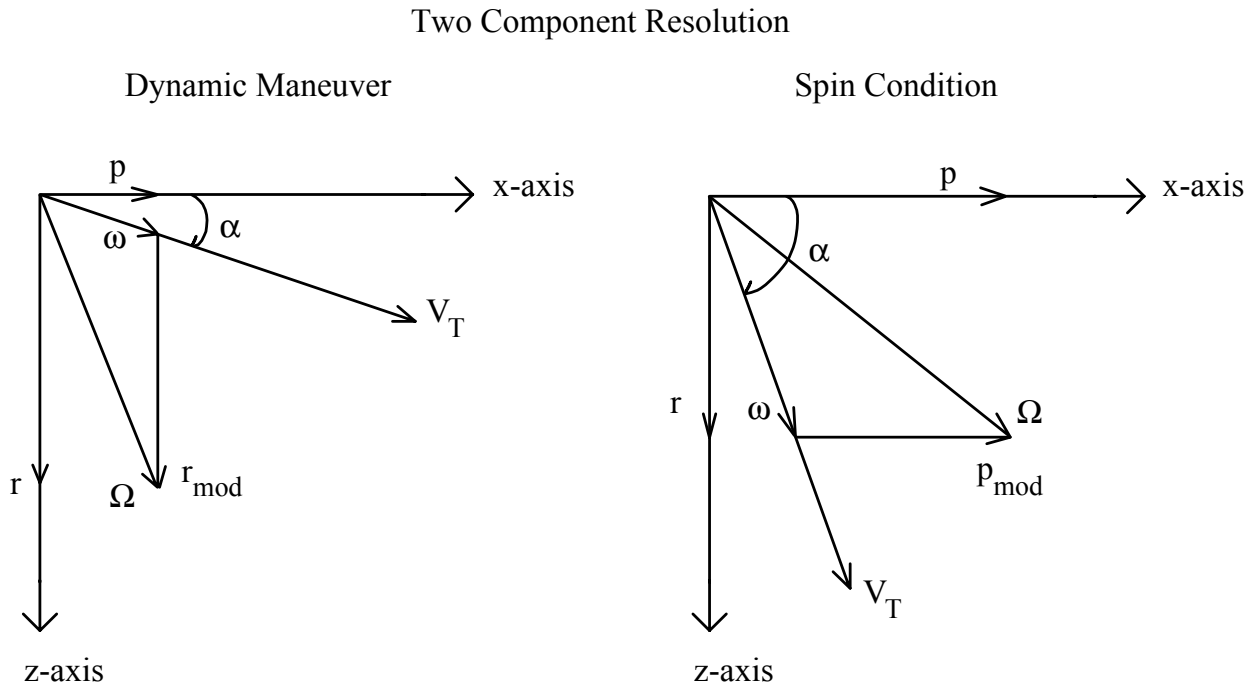

Figure 5. Vector schematic of Kalviste mechanization of dynamic data

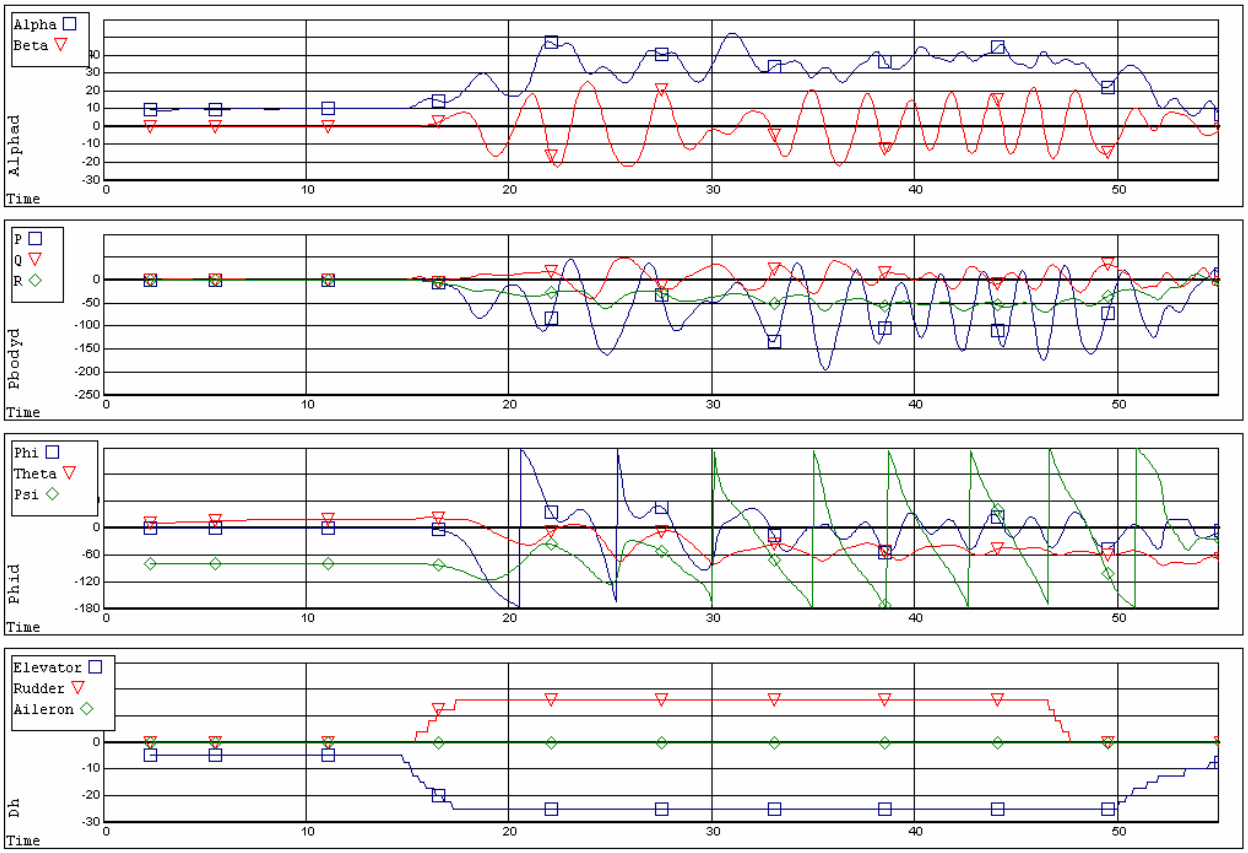

Figure 6. Simulated spin entry and recovery for original configuration.

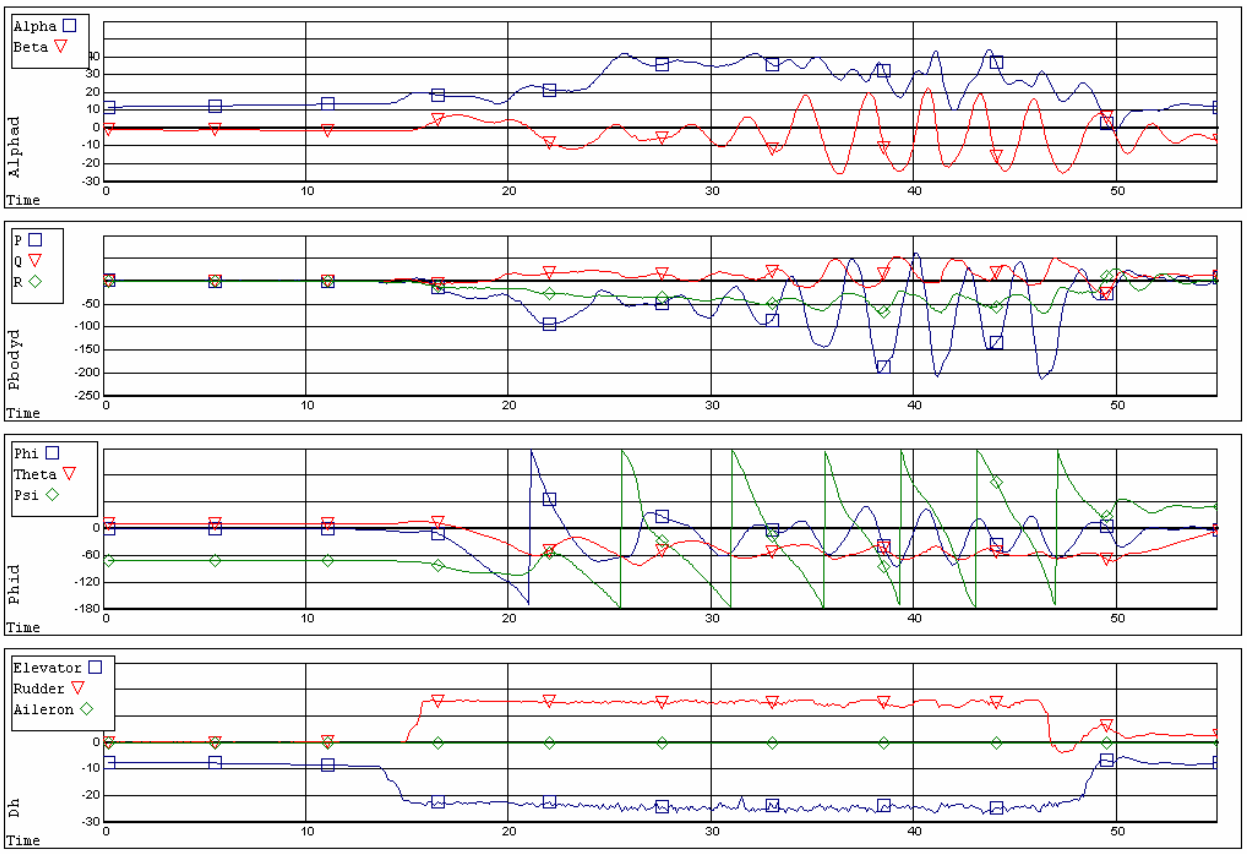

Figure 7. Flight test spin entry and recovery for original configuration.

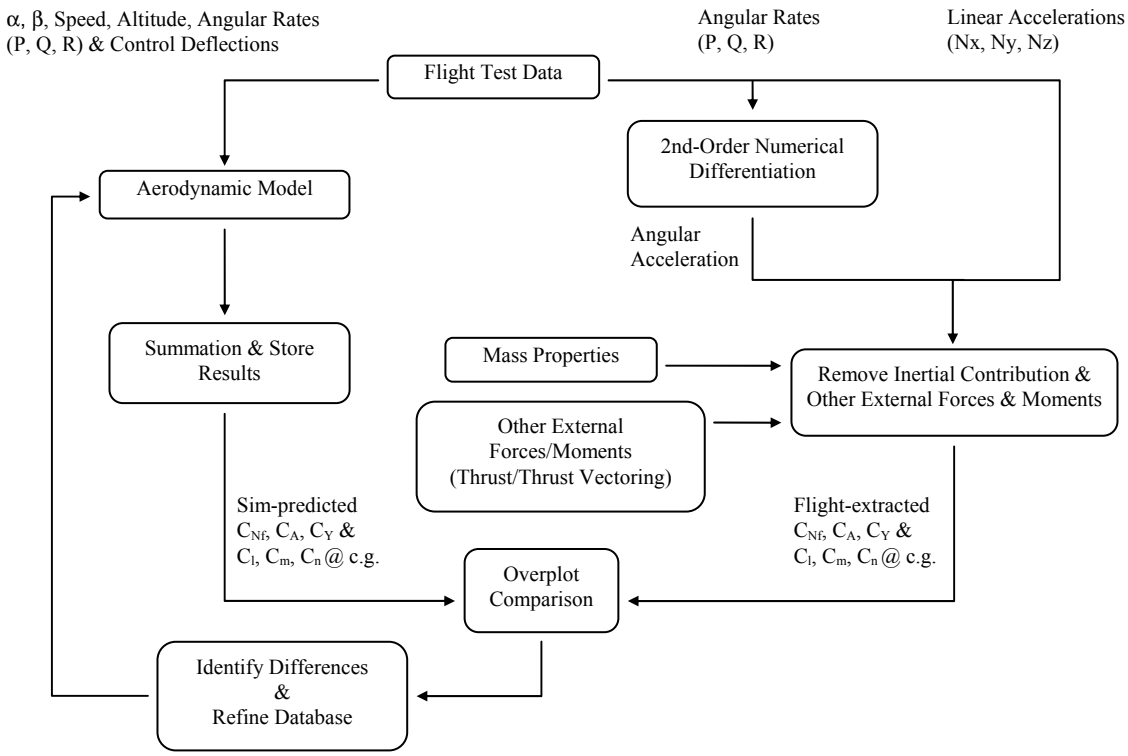

Figure 8. Block diagram of "Overdrive" function

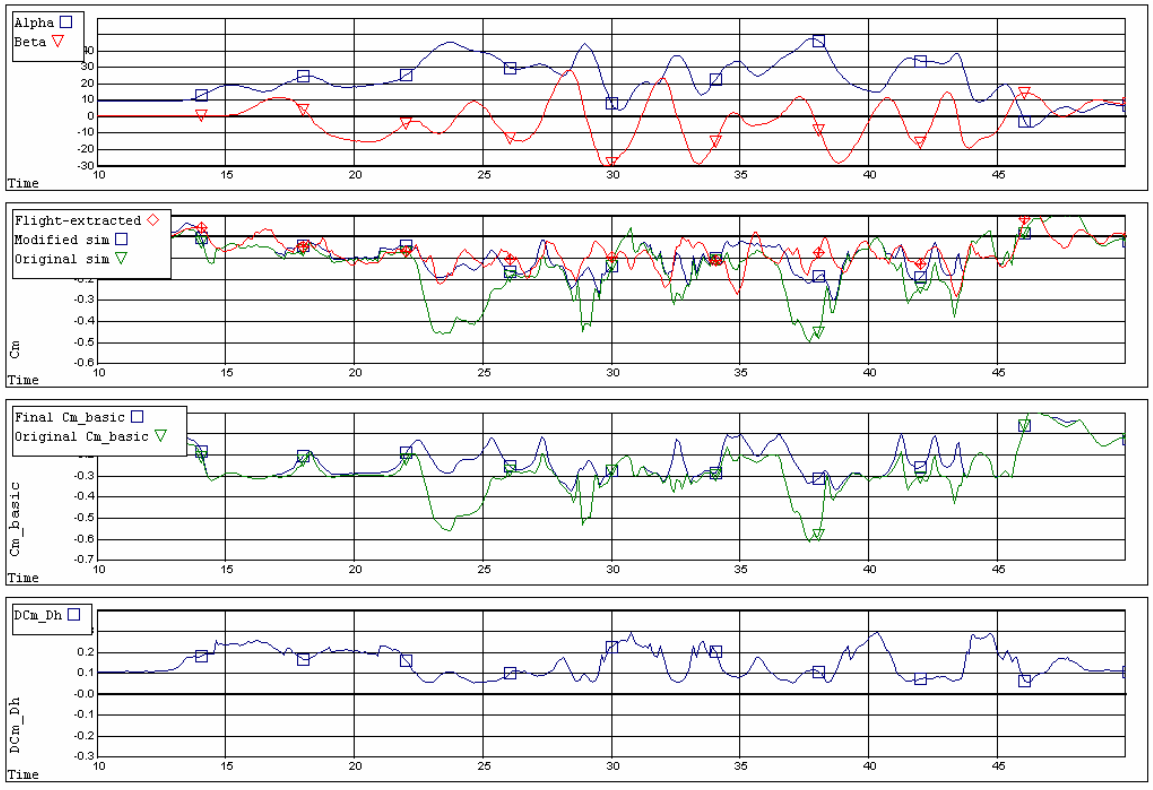

Figure 9. Comparison of simulation and flight-extracted pitching moment.

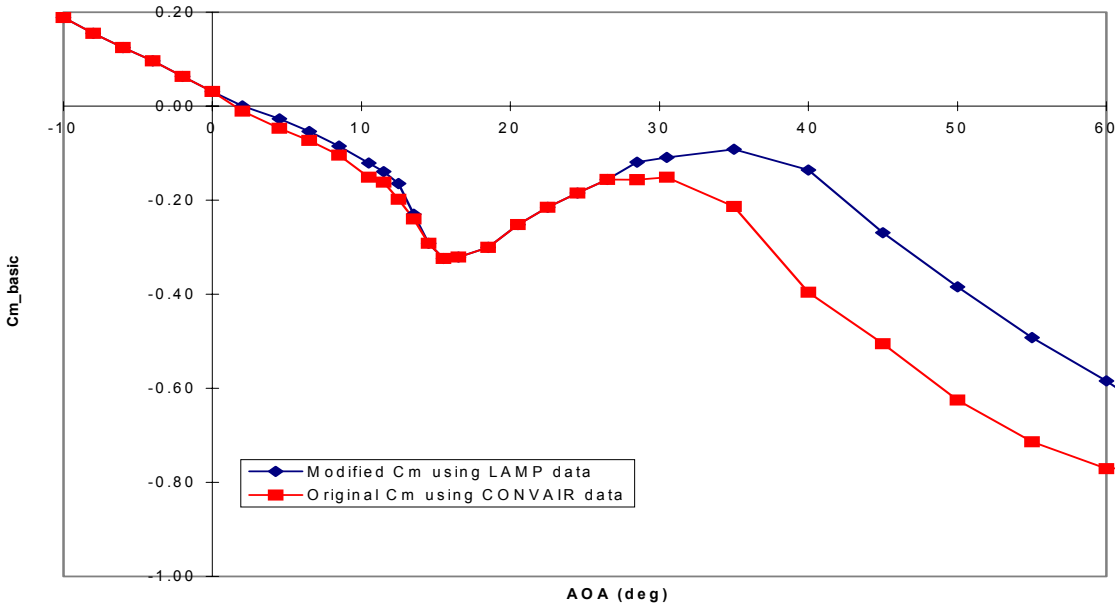

Figure 10. Comparison of CONVAIR & LAMP pitching moment characteristics

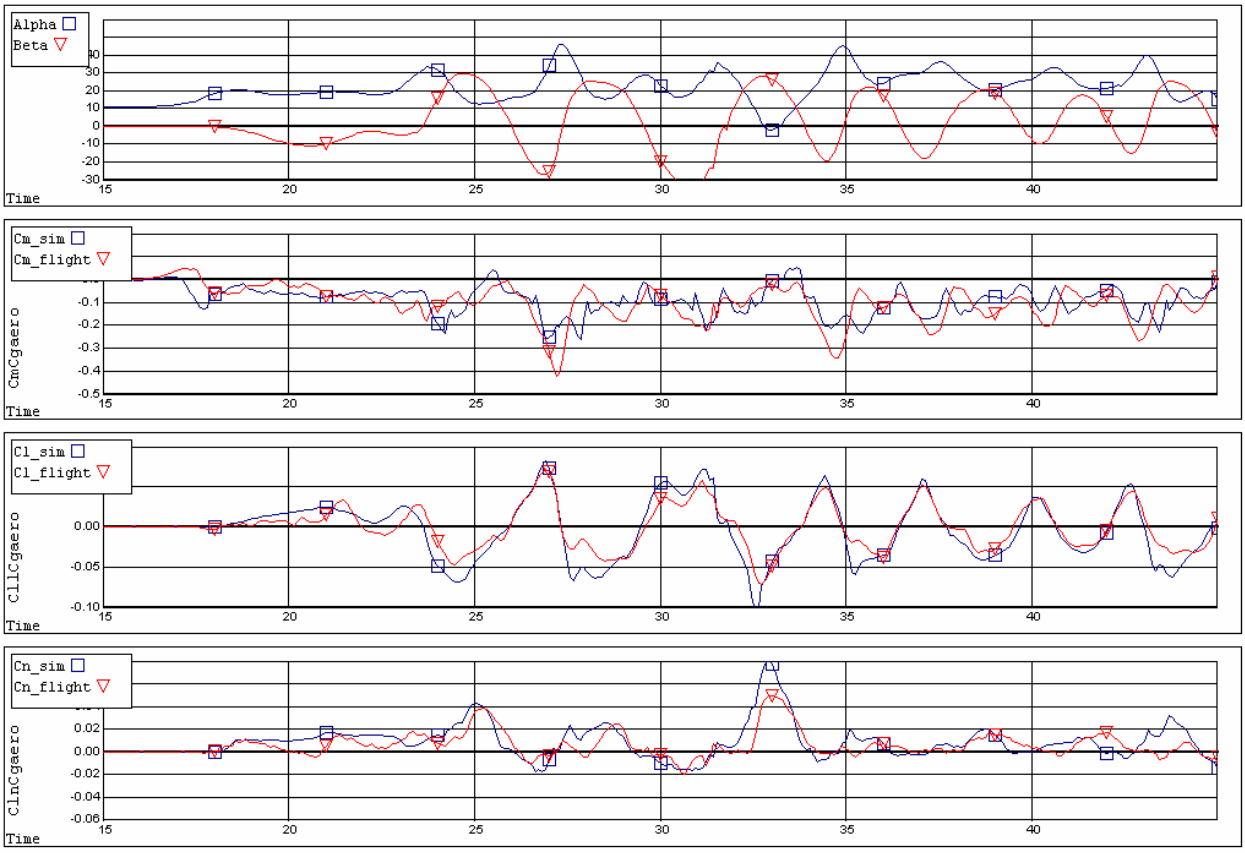

Figure 11. Comparison of simulation and flight-extracted moment coefficients.

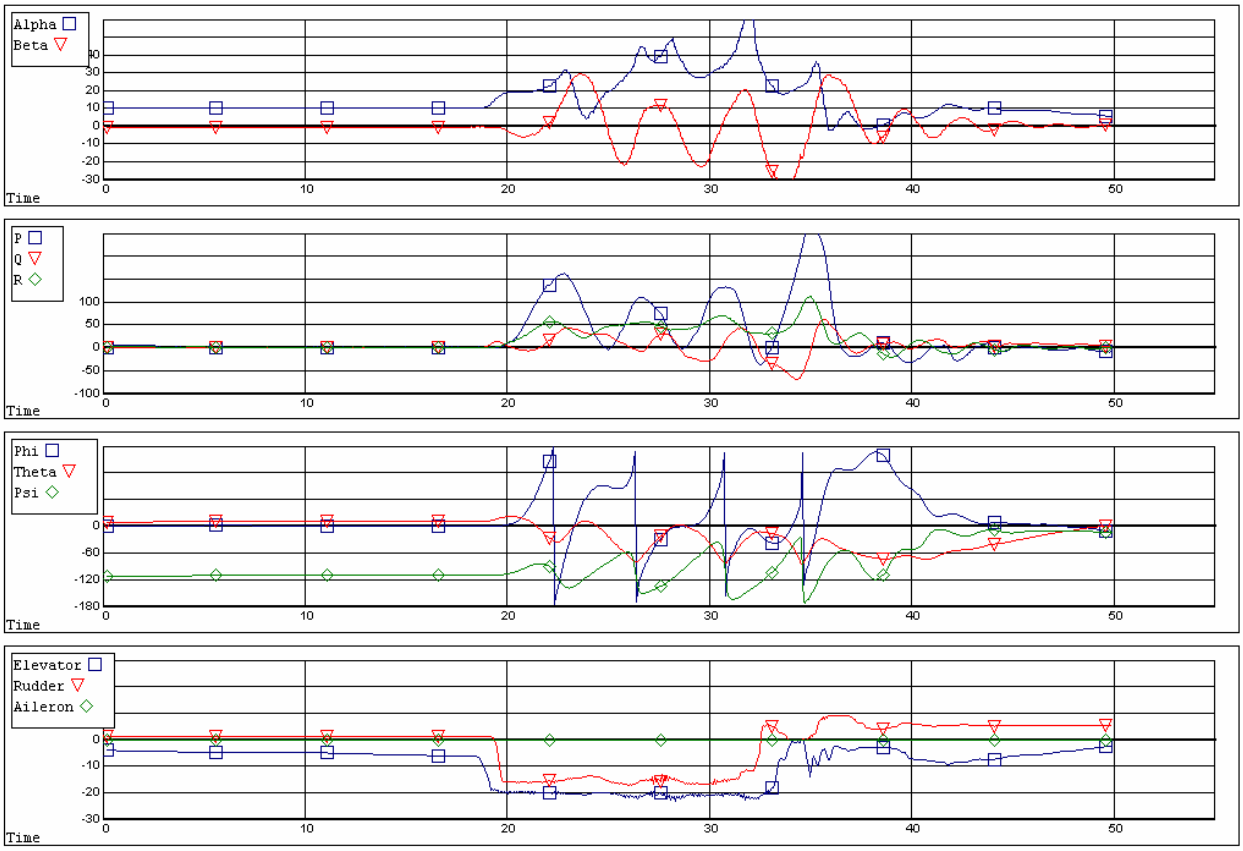

Figure 12. Flight test spin exhibiting "Flick Roll" during recovery.

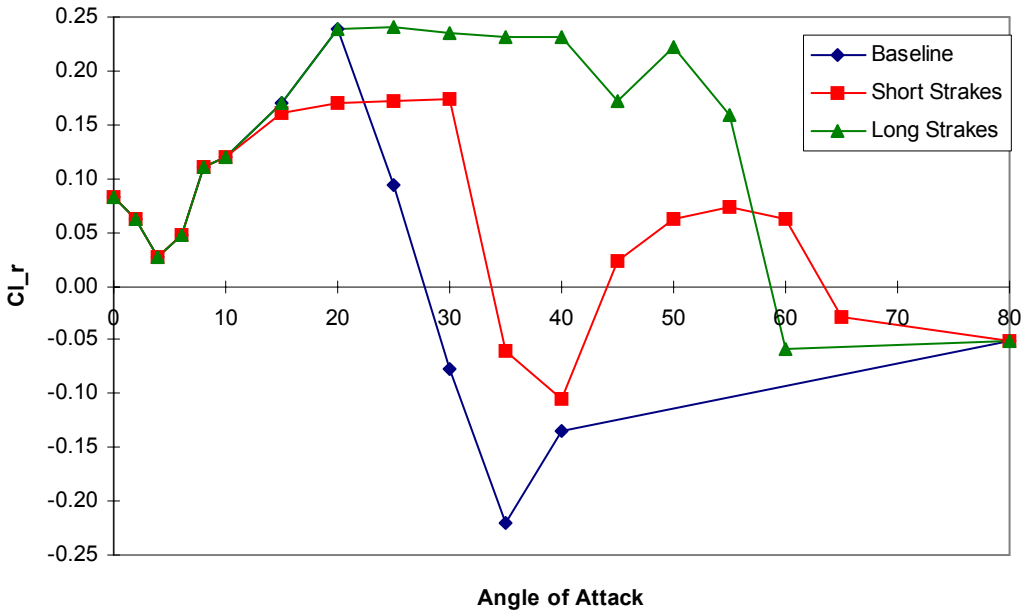

Figure 13. Effect of strakes on rolling moment due to yaw rate (Cl_r)

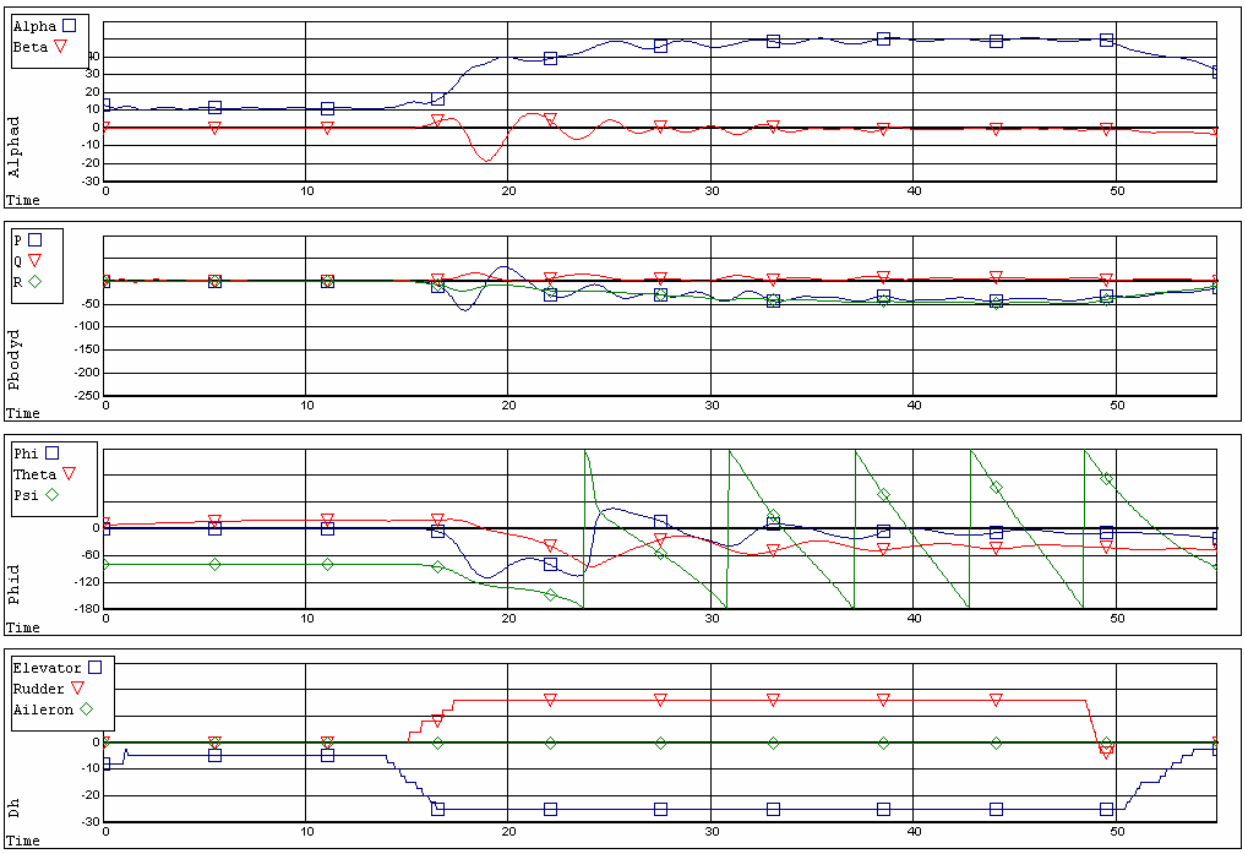

Figure 14. Simulated spin with Clr positive.

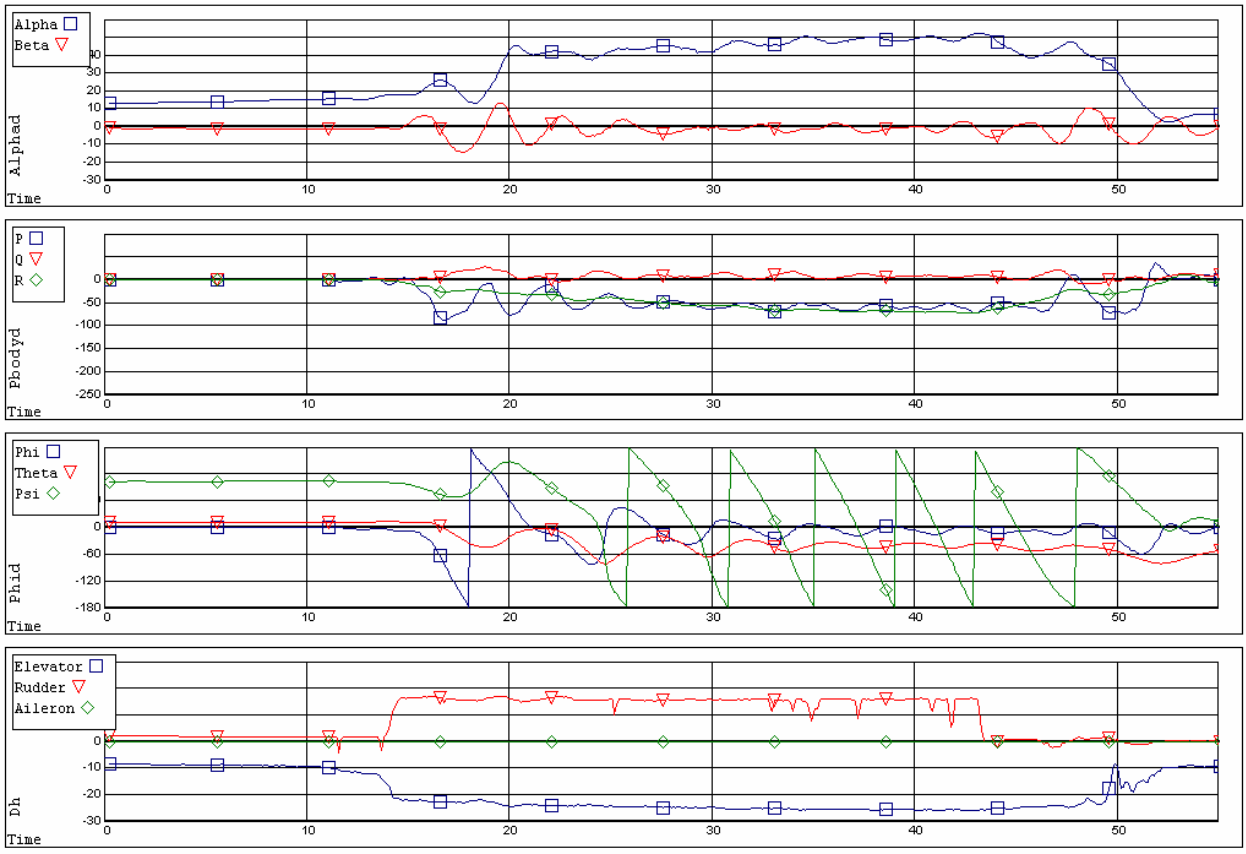

Figure 15. Flight test spin with long strakes.